

Effects of annealing temperature on the formability, mechanical and interface properties of laminated metal composite STS304L/Al1050/STS430

Journal of Composite Materials
2025, Vol. 59(11) 1451–1462
© The Author(s) 2025
Article reuse guidelines:
sagepub.com/journals-permissions
DOI: 10.1177/00219983251314158
journals.sagepub.com/home/jcm



Fabrizio Pertile¹, Samyr Ismail¹, Leonardo M Leidens², Lirio Schaeffer³,
Carlos A Figueroa¹ and Alexandre Fassini Michels^{1,4}

Abstract

Laminated metallic composites (LMCs) produced by cold roll bonding generate high plastic deformation. After the rolling process, it is essential to promote a post-heat treatment (PHT) to increase adhesion, minimize hardening, and enhance the formability of LMCs. In this research, the effects of PHT at low temperatures (250, 350, and 450°C) on LMCs (STS304L/Al1050/STS430) obtained by cold rolling were investigated. The Forming Limit Curve (FLC) and mechanical properties such as ultimate tensile strength (σ_{UT}), yield strength (σ_Y), elongation (ϵ), and the anisotropy index (r -value) of the LMC were evaluated. Results indicate the best PHT temperature that combines formability, increased adhesion between layers, and better mechanical properties, such as elongation (ϵ), which increases from 37% to 55%. At this PHT temperature, the brittle intermetallic layer was not detected, and the FLC showed the best performance. Furthermore, in industrial applications, this PHT condition allows energy savings compared to PHT conditions of high process times (>12 h) and/or temperature (>500°C) reported by several works in the literature.

Keywords

AISI 304L, Al1050, AISI 430, laminated metal composites, cold rolling bonding, forming limit diagram (FLC), mechanical properties, peeling test

Introduction

The use of hybrid materials, also called composite materials, multilayered metal sheets, sandwich metals, or clad metals through multilayers of different constituent materials, has markedly increased year by year. Constituent materials with significantly different chemical and/or physical properties are combined to form a novel material with properties distinct from those of the individual components. The manufacturing of these materials can be accomplished through various methods, including explosion welding, extrusion, drawing, and rolling as pointed out by Rhee et al., and Kim et al.^{1,2} Among these techniques, the cold rolling process distinguishes itself for its high productivity and low production costs as reported by Chaudhari and Acoff,³ and Liu et al.⁴ To guarantee the union of the constituent materials of these laminated metallic composites (LMCs), it is necessary to generate plastic deformations to break the surface oxide layers and promote the adhesion between the

elements as revealed by Manesh and Taheri,⁵ Nagai and Yin, and Mori et al.^{6,7} The plastic deformation fractures the oxide layer and exposes fresh material that subsequently bonds with adjacent interfaces.³

Liu et al. and Wang et al. have shown that plastic deformation simultaneously promotes strain hardening and reduces the formability of LMCs.^{4,8} To minimize such an

¹PPGMAT, Universidade de Caxias do Sul (UCS), Caxias do Sul, Brazil

²IFGW, Universidade Estadual de Campinas (UNICAMP), Campinas, Brazil

³PPG3M, Universidade Federal do Rio Grande do Sul (UFRGS), Porto Alegre, Brazil

⁴PPGMEC, Universidade de Caxias do Sul (UCS), Caxias do Sul, Brazil

Corresponding author:

Alexandre Fassini Michels, PPGMAT, Universidade de Caxias do Sul (UCS), Rua Francisco Getúlio Vargas, 1130, Caxias do Sul 7634, Brazil.

Email: afmichels@ucs.br

Data Availability Statement included at the end of the article

effect and increase the formability, it is necessary to perform a post-heat treatment (PHT) to promote stress relief and the recrystallization of the hardened layer. The PHT can also increase the adhesion between the layers through diffusion between materials. Many studies have evaluated the adhesion and the diffusion of LMCs under process conditions involving high process times (>12 h) as reported by Akramifard et al.⁹ and high process temperatures ($>500^{\circ}\text{C}$) evaluated by Jin and Hong or by Talebian and Alizadeh.^{10,11} As temperatures and durations increase, both factors enhance diffusion,⁶ leading to the formation of a layer of fragile intermetallic compounds at the interfaces of the LMCs as reported by Lee et al., Manesh and Taheri.^{12,13} On one hand, the formation of an intermetallic layer increases the adhesion between the constituent materials,¹¹ but on the other hand, this layer also reduces the formability of the LMCs as shown by Kim and Hong, and Altan and Tekkaya.^{14,15} Therefore, PHT is a critical step in the process,⁹ as the inadequate choice of process parameters can result in the loss of mechanical properties, due to the formation of a layer of brittle intermetallic compounds.^{10,14} Furthermore, the higher process time and temperature lead to increased production costs and energy expenses.

Knowledge of formability is essential to estimate the maximum deformations that the material admits in certain stress states. Sheet metal forming operations can involve complex stresses during part production and the Forming Limit Curve (FLC) serves as a crucial tool for validating various manufacturing processes, notably the deep drawing process. In this context, the validation of the LMC's conformation processes becomes even more important than to a single sheet condition. Due to the fact that the sheets that make up the LMCs, they present have different mechanical properties, distinct anisotropy coefficients, and a complex interface FLC defines the ultimate deformation limits that materials can withstand before experiencing rupture as investigated by Kim et al., and Lu et al.^{16,17}

Despite numerous studies evaluating the properties of LMCs, such as their interfaces as reported by Lee et al., and Kim and Hong,^{12,14} mechanical properties as conducted by Tortorici, and Koseki et al.,^{18,19} or the adhesion characteristics investigated by Akramifard et al., and Abedi and Akbarzadeh,^{9,20} few have assessed their formability. Some studies addressed formability but did not conduct FLC analysis.¹⁴ Other studies^{11,16} conducted FLC analysis but with different constituent materials. In

this research, the FLC and mechanical properties such as ultimate tensile strength (σ_{UT}), yield strength (σ_Y), elongation (ϵ), and the anisotropy index (r-value) of a LMC formed of STS304/Al1050/STS430 were investigated. Additionally, the characteristics of the interface region and the microstructure of these materials before and after a PHT were explored.

Materials and experimental procedures

Materials

The laminated metallic composite (LMC) used in this study was fabricated by Tramontina S.A. through the cold roll bonding process by bonding three distinct materials: stainless steel AISI 304, aluminum alloy 1050, and stainless steel AISI 430, denoted as STS304/Al1050/STS430. The schematic representation of the LMC explored here is illustrated in Figure 1.

The LMC was supplied already bonded in sheets with dimensions of 650.0 mm \times 500.0 mm and a thickness of 2.6 mm. The constituent materials possess individual thicknesses: 0.5 mm for AISI 304, 1.6 mm for Aluminum 1050, and 0.5 mm for AISI 430 (from supplier Aperam South America, Fundaluminio Ltda and Aperam South America respectively). The chemical composition determined through Spark Optical Emission Spectrometry is shown in Table 1.

Experimental procedures

The discussion of the cold rolling parameters falls outside the scope of this work. However, it is important to note that one of the most relevant parameters what governing the bond formation of the LMC layers by rolling is the metals' surface preparation before the rolling process. In this sense, is important degreasing and scratch brushing of aluminum and stainless-steel surfaces creating high bond strength between the layers. After the cold rolling process is important to carry out the PHT process to improve the LMC formability by reducing the work hardening. However, the improper choice of PHT parameters can result in the formation of a layer of brittle intermetallic compounds, leading LMC to loss of formability. Thus, keeping rolling parameters constant, the temperature of the PHT process was varied to observe potential changes in the interface, including the thickness of the diffusion layer and the possible

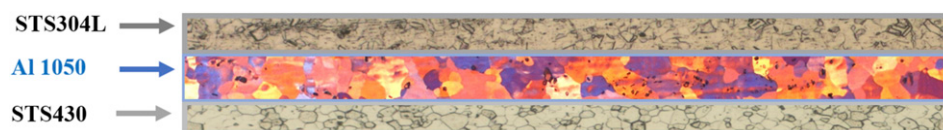


Figure 1. Schematic representation of the LMC used in this study.

Table 1. Chemical composition of constituent materials of LMC used in this study.

STS304L									
Element	C	Mn	Ni	Cr	Mo	Si	P	Al	Fe
Composition %	0.0334	1.07	8.38	18.77	0.137	0.437	0.0252	0.0091	70.2
Al1050									
Element	Al	Si	Fe	Cu	Mn	Mg	V	Ti	Pb
Composition %	99.38	0.113	0.208	0.0393	0.0084	0.0111	0.0056	0.0016	0.2
STS430									
Element	C	Si	Mn	P	Cr	Ni	Nb	Al	Fe
Composition %	0.0267	0.362	0.123	0.0134	16.44	0.103	0.349	0.0041	82.4

formation of intermetallic compounds. The PHT process was carried out at temperatures of 250, 350, and 450°C, with each temperature maintained for 3 hours. For comparison, samples were analyzed in their “non-heat treated” condition, representing the original material “As-Rolled” (AR).

For the investigation of the interfacial properties of the LMC, samples were taken from the cross-sectional area and in the rolling direction, with PHT and AR. The samples were machined and mounted in both conductive and non-conductive epoxy, resin. Metallographic samples were prepared through standard mechanical grinding and polishing on planes perpendicular to the rolling direction. The samples were etched with the Keller reagent, Kroll reagent, and a 2.5 % solution of hydrofluoric acid to observe the microstructure of STS304 L, STS430, and Al1050, respectively. The microstructure and morphology of the samples were observed using an optical microscope (OM) and Field Emission Gun Scanning Electron Microscopy (FEG-SEM Tescan, Mira 3). The elemental chemical composition of the interface and the formation of the diffusion layer between the materials were investigated through energy-dispersive X-ray Spectroscopy line scan analysis (EDS, Oxford Instruments, model SDD X-max 50).

All samples used to evaluate the mechanical properties were taken from the 650.0 mm × 500.0 mm laminated sheets according to the geometry indicated in the respective test standards and were cut using a wire electrical discharge machine (WEDM). The adhesion between the sheet materials STS304/Al1050/STS430 was measured using the peeling test samples according to ASTM D1876-72. The specimens were tested using a Shimadzu AGS-X universal testing machine with a capacity of 100 kN. The peeling strength in terms of N/mm was obtained with a peel rate of 60 mm/min. For all mechanical tests, specimens were taken in three orientations relative to the rolling direction, namely, 0°, 45°, and 90°. The tests were carried out using a universal testing machine, EMIC DL 20000, with a capacity of 200 kN. The procedures and samples were under the ABNT NBR 6892-1 standard. Alongside the tensile test, the values of anisotropy were obtained. To determine the formability

via FLC, the specimens were elongated in the rolling direction of the aluminum, and their geometry included notches ranging from 20 to 200 mm, as shown in Figure S3 of the Supplementary Material. The specimens were electrochemically etched with a square grid pattern with dimensions of 2 mm × 2 mm before being elongated (ISO 12004-1 and ISO 12004-2). Afterward, sheets were fixed on a press with a pressure of 98.07 bar and elongated by a semi-spherical punch of 100.0 mm until the onset of the fracture.

Results and discussion

Metallography and interface analysis

The evaluation of the metallographic structure of the LMCs is shown in Figure 2.

It is possible to observe that there was a great change in the average grain size $13.0 \pm 2.5 \mu\text{m}$ in Figure 2(e) at 350°C, for $16.0 \pm 2.5 \mu\text{m}$ in Figure 2(f) in the condition at 450°C. This growth can be explained by the recrystallization temperature of the Al1050 aluminum alloy, which occurs in the range of 390 to 410°C.²¹ Therefore, in Figure 2(f) the PHT temperature was higher than the aluminum recrystallization temperature, allowing the growth of the material grains as concluded by Chakravarty et al.²²

No significant changes in microstructure were observed for STS304 L, Figure 2(a)–(c), and for STS430, Figure 2(g)–(i). The average grain size in the samples with PHT was $8.5 \pm 2.5 \mu\text{m}$ and in the AR samples, it was $9.0 \pm 2.5 \mu\text{m}$. This phenomenon is explainable considering the recrystallization temperatures for STS304 L and STS430 steels are 1010°C to 1120°C and 760°C to 815°C, respectively.

The diffusion layer was investigated at the LMCs' interfaces via Energy-Dispersive X-ray Spectroscopy (EDS) line scan analysis and by Scanning Electron Microscopy (SEM) analysis. Figure 3(a)–(f) show the combination of SEM images with line chemical analysis of the region via EDS carried out at the LMCs interfaces. The AR samples are shown in Figure 3(a) and (d), the PHT at 350°C in Figure 3(b) and (e) and the PHT at 450°C in Figure 3(c) and (f).

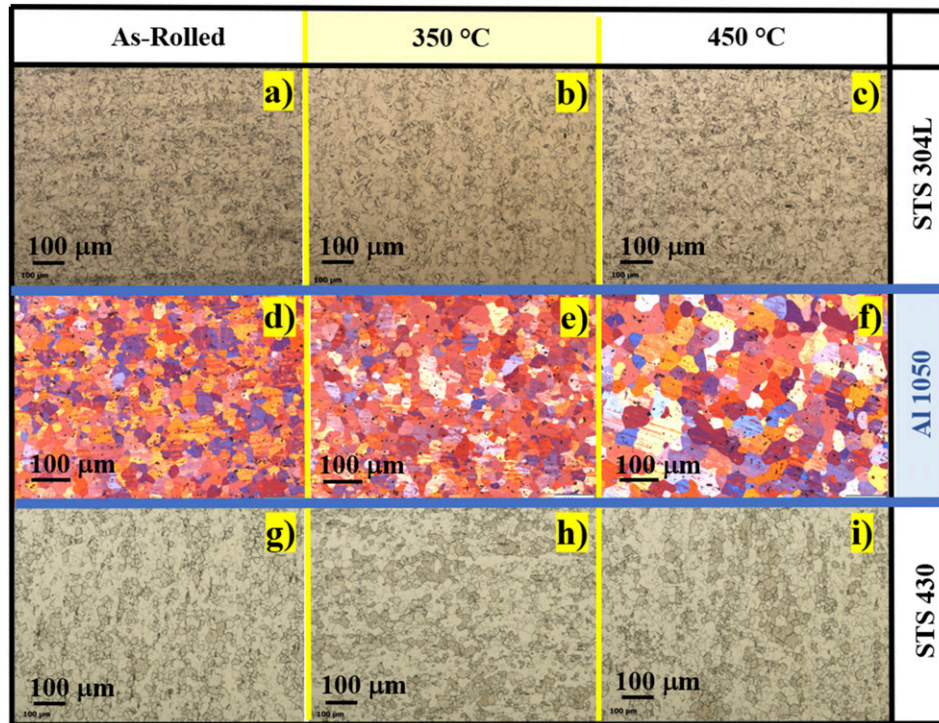


Figure 2. Metallography of STS304 L stainless steel (a) non-heat treated, (b) heat treated at 350°C and (c) at 450°C; Al1050 (d) non-heat treated, (e) heat treated at 350°C and (f) at 450°C; STS430 stainless steel (g) non-heat treated, (h) heat treated at 350°C and (i) at 450°C.

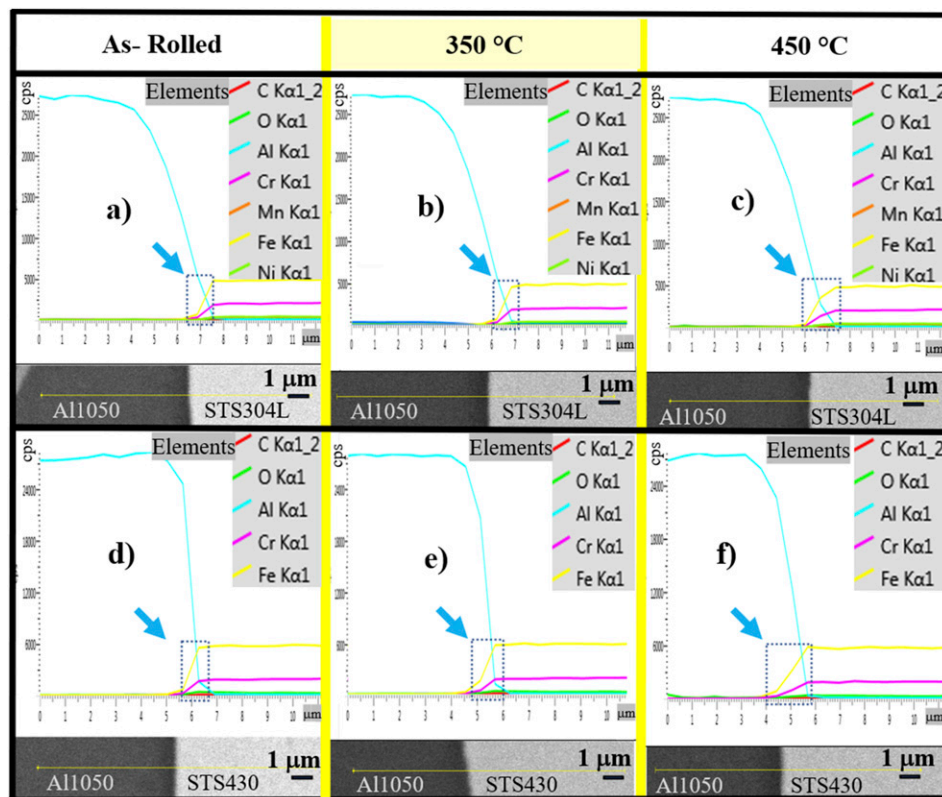


Figure 3. SEM images and EDS line scan analysis profiles near the interface between Al1050/STS304 L and Al1050/STS430, without heat treatment (a) and (d), heat treated at 350°C (b) and (e); and at 450°C (c) and (f).

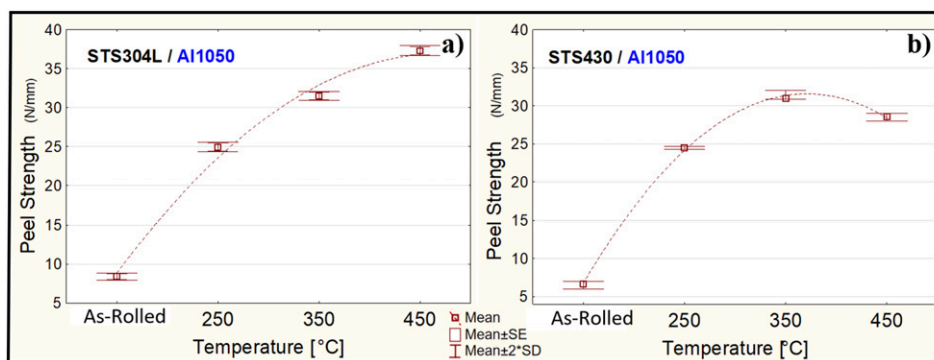


Figure 4. Graph peel strength versus heat-treated conditions.

The literature shows an intermetallic layer with micrometric thickness but at higher temperatures than used in this work.^{1,9} It is not possible to observe the formation of a micrometric intermetallic layer for any PHT temperatures in the SEM images, as we can see in Figure 3 or in original figures Figures S1 and S2. In contrast to previous studies, which employed temperatures as high as 550°C for up to 44 hours¹⁴ or 600°C for up to 48 hours,¹⁸ this study utilized lower temperatures (250, 350, and 450°C) and shorter durations, with a maximum of 3 hours. However, it is possible to observe changes in the chemical concentrations at the interfaces (Fe and Al) in the line scan analysis images via EDS, which were indicated by arrows and a dashed line box within the figures. One can see the box pointed out by dotted lines in Figure 3(c) and (f) indicate increased diffusion due to the lower slope of element profiles, which is consistent with the higher temperatures of the PHT (450°C). The diffusion of interstitial elements in the interface region signals the onset of an intermetallic layer. While, on the one hand, the presence of the intermetallic layer enhances adhesion,⁸ on the other hand, its presence is not advantageous for component formability.^{13,14} Hence, investigating the interface adhesion and formability of LMCs becomes imperative.

Adhesion

The adhesion between the layers of the constituent materials was quantitatively evaluated through the T-peeling test, described in Supplementary Material (Figure S4). The graph in Figure 4 displays the results of the average peel strength (N/mm) required for the detachment of the STS304 L/Al1050 and STS430/Al1050 joints at each PHT temperature. It is possible to observe that an increase in temperature leads to an increase in adhesion. For the STS304 L/Al1050 interface, the adhesion starts with a peel strength of 8.36 N/mm for the AR samples, reaching 37.37 N/mm in samples subjected to a 450°C PHT. As for the STS430/Al1050 interface, the adhesion starts with a peel

strength of 6.65 N/mm for the AR samples, reaching values of 28.53 N/mm in samples subjected to a 450°C PHT. The maximum peel strength reached between 350°C and 450°C for the STS430/Al1050 interface may be associated with the competitive mechanisms of a thicker diffusion interface and microstructural modifications near the interface.

Due to the greater mobility of interstitial atoms with increasing temperature, the diffusion layer between the materials grows, leading to an increase in adhesion between the layers of the constituent materials. Therefore, the increase in adhesion can be attributed to the formation of a diffusion layer in the region of the interfaces. Similar behavior was observed in the literature for the three-layered St/AZ31/St.²⁰

Mechanical properties

From the tensile test, the values of ultimate tensile strength (σ_{UT}), yield strength (σ_Y), elongation (ϵ), and anisotropy index (r -value) were obtained and are presented in Table 2. Using the data from the true stress-strain curve (true stress (σ) versus true strain (ϕ), as shown in Figure 5, the Holloman equation ($\sigma = K\phi^n$) was fitted, resulting in the determination of Mean and Standard deviation (S_x) of the strain-hardening exponent (n) and the strength coefficient (K), also displayed in Table 2.

It is possible to observe in Table 2 that in the 0° rolling direction, the yield strength (σ_Y) was significantly affected during the PHT, which is consistent with the metallographic analysis of the work-hardened layer of Al1050. The anisotropy coefficient is higher in the direction of 45° relative to the rolling direction. This result is consistent with previous studies that reported higher anisotropy values at angles exceeding 45° relative to the rolling direction.¹⁶ Considering the anisotropic nature of the LMC, as the r -value is different from 1, this study utilized the average of the three rolling directions to evaluate the mechanical properties shown in Figures 5 and 6.

Table 2. Engineering stress-strain data (σ_{UT} , σ_Y , ϵ , r-value) and Holloman equation constant (n and K) according to the temperature and sample removal direction in relation to the rolling direction.

Tempe-rature	Direction	σ_Y [MPa]	σ_{UT} [MPa]	Elongation ϵ [%]	Anisotropy Index (r-value)	n [-]	K [MPa]
As-Rolled	0°	241.00	278.00	39.50	0.63	0.102	389.00
	45°	256.00	274.00	37.50	0.88	0.096	376.18
	90°	258.00	278.00	35.50	0.70	0.132	371.75
	Mean	252	277	37	0.74	0.110	379
	S_x	9	2.3	2	0.13	0.020	9
250°C	0°	199.00	261.00	47.00	0.72	0.139	394.21
	45°	210.00	258.00	43.50	0.99	0.125	378.98
	90°	209.00	259.00	48.00	0.85	0.130	371.75
	Mean	206	259	46	0.85	0.130	386
	S_x	6	1.5	2.3	0.14	0.010	11.5
350°C	0°	186.00	261.00	55.40	0.78	0.154	406.80
	45°	191.00	257.00	49.00	0.97	0.139	387.36
	90°	189.00	256.00	57.80	0.81	0.146	371.86
	Mean	189	258	54	0.88	0.146	395
	S_x	2.5	2.6	4.5	0.10	0.010	17.5
450°C	0°	178.00	261.00	54.40	0.78	0.154	406.20
	45°	182.00	258.00	53.80	1.14	0.144	392.82
	90°	179.00	255.00	55.80	0.82	0.154	402.41
	Mean	180	258	55	0.91	0.151	400
	S_x	2	3	1	0.20	0.010	6.9

As can be observed in Figure 5, the increase in PHT temperatures altered the mechanical properties of the LMC. The Yield Strength (σ_Y) decreased by 28.6 %, from 252 to 180 MPa, and the Ultimate Tensile Strength (σ_{UT}) decreased by 6.8 %, from 277 to 258 MPa. Conversely, the elongation (ϵ) experienced an increase of 31.3 %, rising from 37.5 % to 54.67 %. A similar behavior was observed in the literature for σ_{UT} and ϵ of stainless steel/aluminum/copper clad-metal sheets at annealing temperatures of 100 to 400°C.¹² However, it can be noted that there was a

stabilization of these properties between the temperatures of 350 to 450°C. This phenomenon was also detected in the literature in the manufacturing of a multilayered composite (Al-1100/St-12/Al-1100) by accumulative roll bonding and subsequent annealing. In this case, the strength of the composite remains approximately constant after annealing between 300°C and 400°C.¹¹ The evolution of mechanical properties with increasing temperature can be attributed to stress relief and recrystallization of Al1050 during the PHT, eliminating some of the cold rolling work hardening.

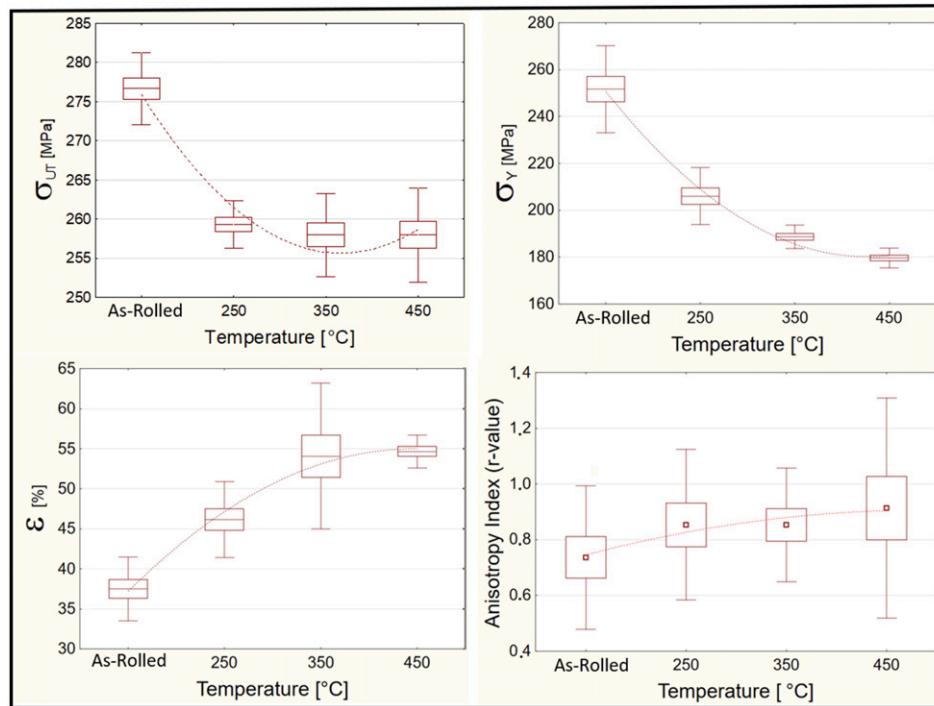


Figure 5. Experimental mechanical properties of the LMCs versus heat treated: (a) ultimate tensile strength (σ_{UT}), (b) Yield strength (σ_Y), (c) elongation (ϵ), and (d) anisotropy index (r-value).

Additionally, the increased adhesion between aluminum and stainless steel may also play a role in the variations of mechanical properties.

It is also possible to observe an increase in the trend line of the average anisotropy index from 0.74 in the ‘non-heat treated’ samples to 0.91 in the samples subjected to PHT at 450°C. Therefore, the PHT allowed the LMCs to approach the isotropic condition when the r-value = 1.

Figure 6 shows the stress-strain curves in the longitudinal direction of rolling (0°), where it is possible to observe the maximum elongation of the material subjected to PHT at 350°C.

Based on the obtained values, it is possible to observe in Figure 6(b) an increase in the strain-hardening exponent (n) as the PHT temperature increases,¹⁵ while the mean strength coefficient (K) shows no significant change. The increase in (n) indicates that, under uniaxial tension conditions, the material enhances its deformation capacity ϵ , as shown in Figure 5(c). However, the (n) value remained below that of the annealed Al1050 aluminum alloy. Regarding the strength coefficient in Figure 6(c) and the mechanical properties (σ_{UT} , σ_Y , ϵ), they exhibited intermediate performance between Al1050 aluminum and annealed STS304 L and STS430 steels, similar behavior has been found by Jin and Hong¹⁰ involving multilayer sheets of Al3003/SS439 or by Gu et al. for Al1050/low-carbon steel/Al1050 layered sheet.²³ However, there were no remarkable changes in microstructure and mechanical properties when

ST306 L sheets were individually heat-treated at 600°C for 2 h.²⁴

A summary of all the mechanical properties of the forming materials as well as of the LMC at different PHT temperatures is shown below in Table 3.

As stress is applied, the lower-strength material (Al1050) begins to deform plastically and work-hardened. Subsequently, failure initiates in Al1050 and progresses to stainless steels STS304 L and STS430. This failure occurs due to the presence of a stress concentrator, even when the stress is below the ultimate tensile strength of the stainless steels. This phenomenon was also observed in the study with multilayer steels for improved combinations of high strength and high ductility.^{19,20,25} Previous studies on a Copper/Steel/Copper clad plate indicated that with the increase in loading force, many shear bands and voids are formed. The clad plate is then thinned, while the steel substrate fractures due to the convergence and growth of voids.⁴

Formability

Considering that typically in practical processes of forming parts, failure occurs in distinct states from the biaxial deformation condition, it is crucial to evaluate alternative stress conditions, like plane and uniaxial strain, as provided by the Forming Limit Curve (FLC). In this work, for formability evaluation via FLC, specimens of LMCs

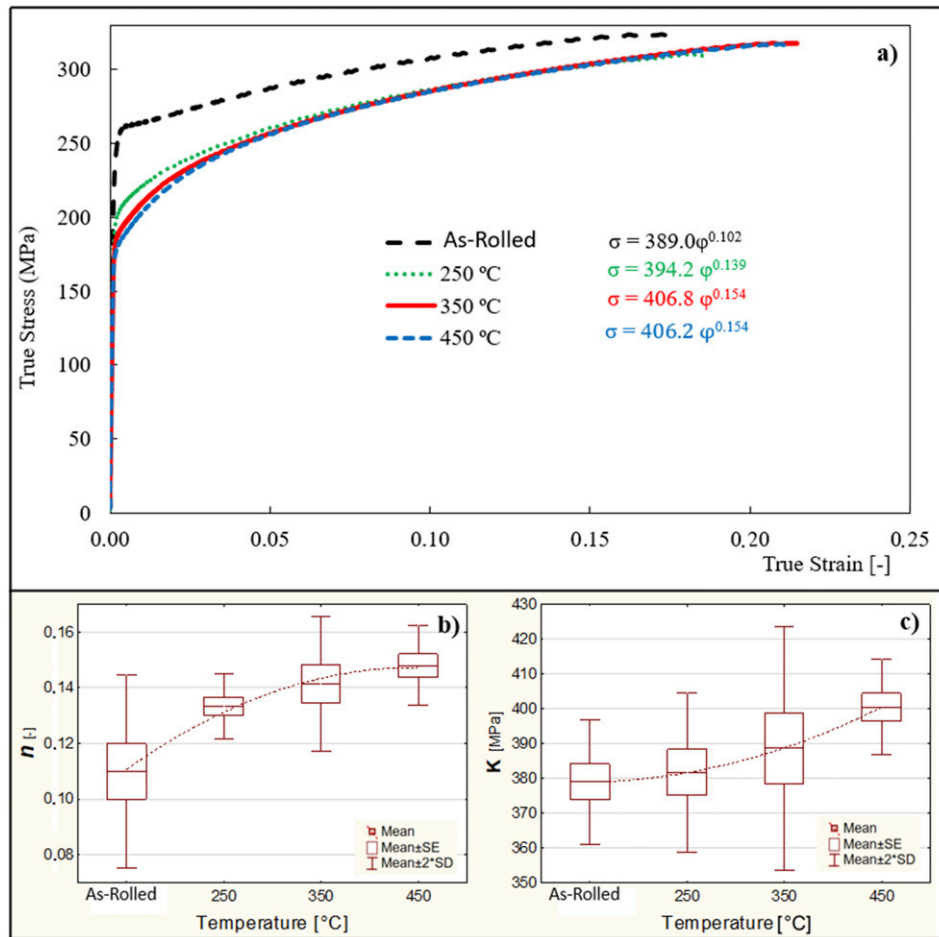


Figure 6. Experimental mechanical properties of the LMCs in the AR condition and with PHT at 250, 350, and 450°C: (a) True stress versus true strain graph, specimen taken in the rolling direction (0°), (b) Mean of strain-hardening exponent (n) and (c) Mean strength coefficient (K).

Table 3. Mechanical properties of the constituent materials and the LMC used in this work (AR and in the PHT condition).

Material	σ_Y [Mpa]	σ_{UT} [Mpa]	Elongation ϵ [%]	n [-]	K [Mpa]
STS304 L	269	1006	63	0.367	1227
Al1050	53	91	29	0.151	120
STS430	337	477	30	0.236	973
STS304/Al1050/STS430 As-Rolled	252	277	37	0.110	379
STS304/Al1050/STS430 (250°C)	206	259	46	0.130	386
STS304/Al1050/STS430 (350°C)	189	258	54	0.146	395
STS304/Al1050/STS430 (450°C)	180	258	55	0.151	400

detailed in Figure S3 were elongated as depicted in Figure 7. For all specimens the dimensions of the square grid were evaluated from the original dimensions before deformation, close to the region of maximum deformation (highlighted, for example, in the red boxes in Figure 7). It is also possible to observe, in the region near the crack, that the square grid

presents distinct deformations comparison to region of minimum deformation shown in blue box detail.

In general, fracture details indicated that the crack extends according to the criterion of the maximum main stress. Compared with previous work,²⁶ it is possible to state that the annular cracks of LMCs with a sawtooth shape

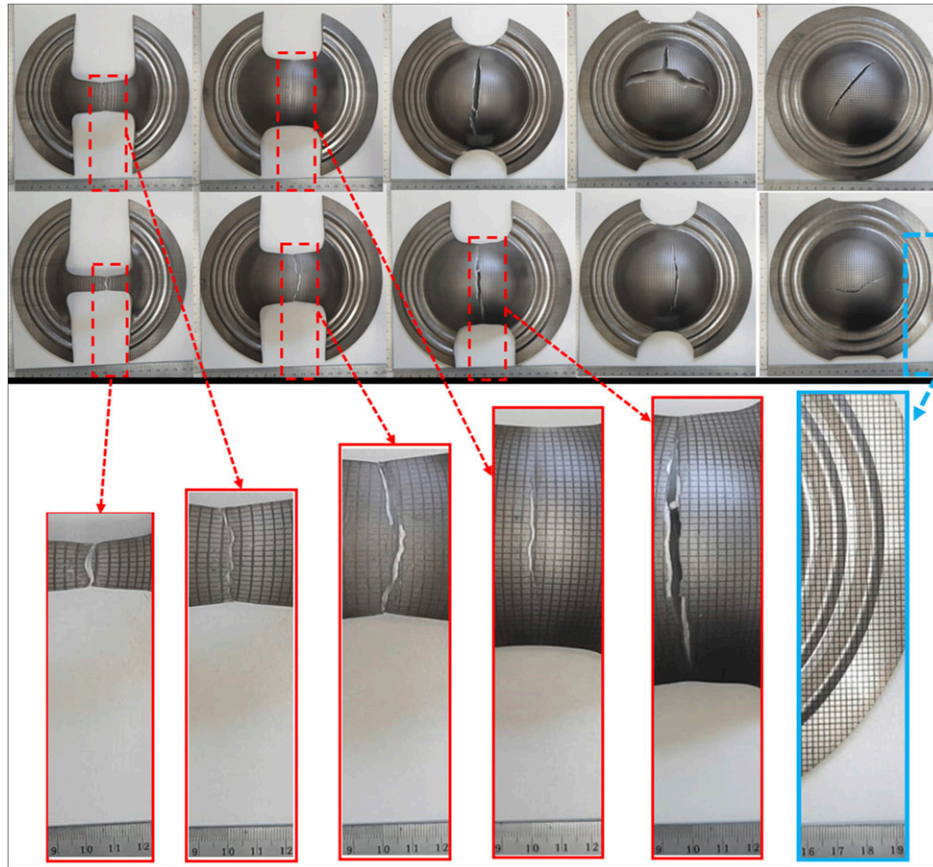


Figure 7. Deformation results of LMCs specimen's whit PHT at 350°C and details of region of maximum and minimum deformation.

characteristic are typical of a ductile fracture, distinctly from a brittle mostly straight. Therefore, for any PHT temperatures, the specimens presented similar characteristics of a typical ductile fracture.

Figure 8 illustrates the FLC of the samples with the PHT at 350°C. For the construction of the FLC, a major strain (ϕ_1) was plotted along the Y-axis, and the minor strain (ϕ_2) was plotted along the X-axis.

Figure 9 displays the FLCs of samples subjected to PHT at 250, 350, and 450°C, as well as the AR condition. It is noticeable in the biaxial strain region that the higher the PHT temperature, the lower the material formability. Similar behavior has been observed in the literature for biaxial stress conditions using the Erichsen cupping test technique on heat-treated Al-clad steel sheets (1050/St37) in the temperature range of 450 to 525°C for 3 hours. This phenomenon was attributed to static strain aging of the Al-clad steel sheet at an annealing temperature below 525°C.^{5,13}

In the plane strain condition, it is possible to observe that the 450°C PHT temperature shows minimum values of the maximum principal strain (ϕ_1), indicating lower formability. It is also possible to observe in plane strain that,

within experimental uncertainties, there are no significant differences between the PHT conditions at 250°C and 350°C. This behavior can also be observed for the biaxial strain condition. It is possible to verify that the AR condition exhibits higher formability under plane and biaxial strain conditions compared to the PHT samples. However, due to the low adhesion evidenced in the peeling test (Figure 4), the AR condition is highly susceptible to generating delamination between the layers of the LMCs in practical forming processes.

Observing Figure 9 in the uniaxial strain region, within the experimental uncertainty, the PHT at a temperature of 350°C showed a tendency to displacement of the FLC in the positive direction of the ϕ_1 axis. This displacement demonstrates greater formability under this stress condition. These results agree with the tensile test results presented in Figure 6 and with the mechanical properties of the LMCs shown in Figure 5. Therefore, despite the treatment at 450°C showing better adhesion between the layers (Figure 4), this PHT condition exhibited lower formability in all regions of the FLC. These data are consistent with SEM electron microscopy images, which indicated the onset of formation of a layer of brittle intermetallic compound that reduces

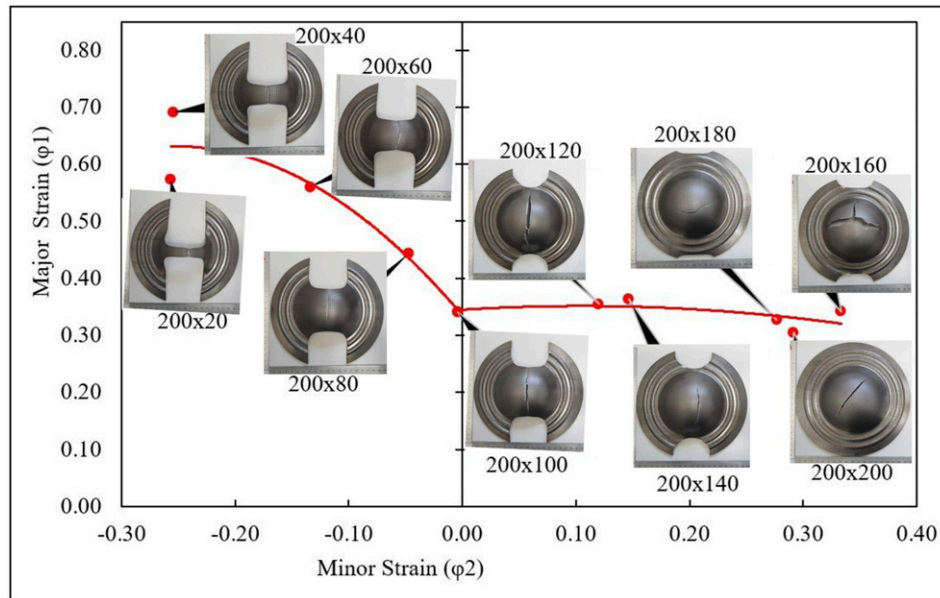


Figure 8. Distribution of samples in the FLC according to their geometry.

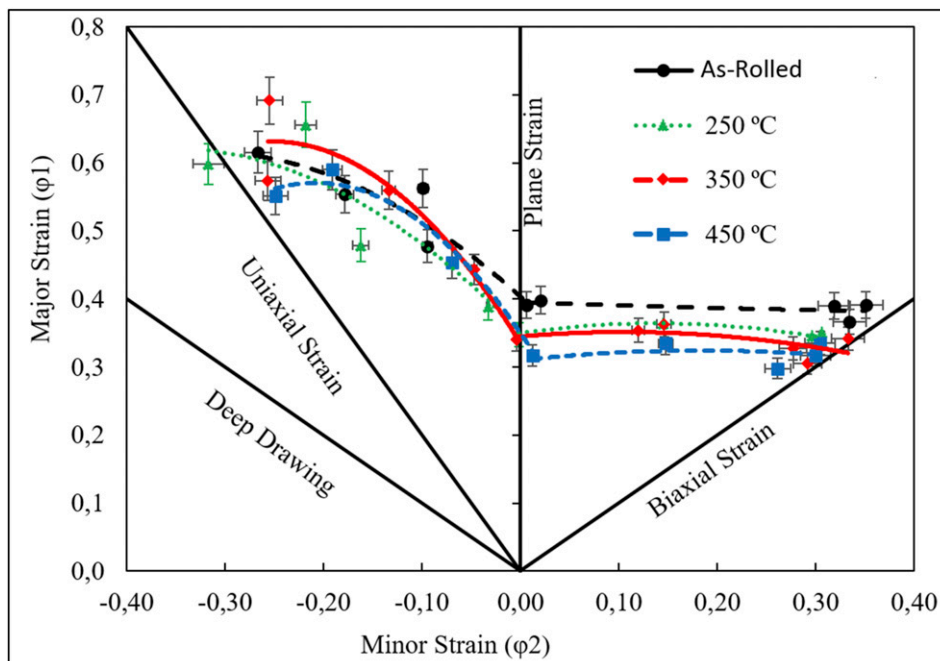


Figure 9. Forming Limit Curve (FLC) with heat-treated specimens at different temperatures.

formability.^{5,13} Furthermore, PHT at 450°C implies an increase in the energy consumption of the production processes in the manufacturing of LMCs parts compared to PHT at 350°C. It is concluded that the PHT condition at 350°C exhibits the best balance among adhesion between layers, mechanical properties, and formability of STS304/AI1050/STS430 LMCs.

Conclusions

In this study, the effect of PHT at temperatures of 250, 350, and 450°C on the formability of the STS304/AI1050/STS430 LMC was examined through the analysis of FLC, mechanical properties, interface analysis, and metallography. The results are summarized below:

1. The increase in PHT temperature resulted in enhanced adhesion between the layers, promoting recrystallization only in the Al1050 layer and altering the mean anisotropy index (r-value) from 0.74 to 0.91.
2. With the increase in PHT temperature, an enhancement of mechanical properties such as elongation (ϵ), from 37 to 55 %, and the strain-hardening exponent (n), from 0.102 to 0.154 was observed. Conversely, ultimate tensile strength (σ_{UT}) and yield strength (σ_Y) exhibited the opposite behavior, reducing their values with the increase in PHT temperatures. Within the experimental uncertainties of the study, it was possible to observe that between PHT temperatures of 350 and 450°C, mechanical properties remained stable.
3. At the PHT at 450°C, a change was observed in both STS/Al interfaces, indicating the onset of the formation of a brittle intermetallic compound that altered the formability of the LMCs, as shown in the FLC.
4. Among all the samples in the study, the 350°C PHT showed the best balance among mechanical properties, adhesion between layers, and the best performance in the FLC. Furthermore, the PHT at 350°C allows for a reduction in energy consumption compared to the PHT at 450°C.
5. From an industrial perspective, this study allows the definition of the PHT temperature that combines mechanical properties, adhesion between constituent materials, and formability with production conditions of lower energy consumption in the manufacturing of LMCs parts.

Acknowledgments

The authors C.A.F. and A.F.M. are grateful to CNPq or CAPES fellows. This work was financially possible due to the following projects: INCT-CNPq (#308567/2018-8), FAPERGS (#19/2551-0000656-0 and 19/2551-0002288-3). L. M. L. is a FAPESP fellow (grant 2023/07552-0). The authors would like to thank LCMIC colleagues and Dr F. P. Missell for their support during this research by the LCM lab.

Declaration of conflicting interests

The author(s) declared no potential conflicts of interest with respect to the research, authorship, and/or publication of this article.

Funding

The author(s) disclosed receipt of the following financial support for the research, authorship, and/or publication of this article: This work was supported by the Conselho Nacional de Desenvolvimento Científico e Tecnológico (CNPq 309188/2021-0), Centros de Pesquisa, Inovação e Difusão, Fundação Amazônia Paraense de

Amparo à Pesquisa fellow (grant 2023/07552-0), INCT-CNPq (#308567/2018-8), FAPERGS (#19/2551-0000656-0 and 19/2551-0002288-3).

ORCID iD

Alexandre Fassini Michels  <https://orcid.org/0000-0002-0570-5320>

Data availability statement

Data sharing not applicable to this article as no datasets were generated or analyzed during the current study.

Supplemental material

Supplemental material for this article is available online.

References

1. Rhee KY, Han WY, Park HJ, et al. Fabrication of aluminum/copper clad composite using hot hydrostatic extrusion process and its material characteristics. *Mater Sci Eng* 2004; 384: 70–76. DOI: [10.1016/j.msea.2004.05.051](https://doi.org/10.1016/j.msea.2004.05.051).
2. Kim JK, Huh MY, Lee JC, et al. Evolution of strain states and textures during roll-cladding in STS/Al/STS sheets. *J Mater Sci* 2004; 39: 5371–5374. DOI: [10.1023/B:JMSC.0000039247.10346.5d](https://doi.org/10.1023/B:JMSC.0000039247.10346.5d).
3. Chaudhari GP and Acoff V. Cold roll bonding of multi-layered bi-metal laminate composites. *Compos Sci Technol* 2009; 69: 1667–1675. DOI: [10.1016/j.compscitech.2009.03.018](https://doi.org/10.1016/j.compscitech.2009.03.018).
4. Liu BX, Wei JY, Yang MX, et al. Effect of heat treatment on the mechanical properties of copper clad steel plates. *Vacuum* 2018; 154: 250–258. DOI: [10.1016/j.vacuum.2018.05.022](https://doi.org/10.1016/j.vacuum.2018.05.022).
5. Manesh HD and Taheri AK. Bond strength and formability of an aluminum-clad steel sheet. *J Alloys Compd* 2003; 361: 138–143. DOI: [10.1016/S0925-8388\(03\)00392-X](https://doi.org/10.1016/S0925-8388(03)00392-X).
6. Li L, Nagai K and Yin F. Progress in cold roll bonding of metals. *Sci Technol Adv Mater*. 2008; 9: 1. Article 023001. doi:[10.1088/1468-6996/9/2/023001](https://doi.org/10.1088/1468-6996/9/2/023001).
7. Mori KI, Bay N, Fratini L, et al. Joining by plastic deformation. *CIRP Ann Manuf Technol* 2013; 62: 673–694. DOI: [10.1016/j.cirp.2013.05.004](https://doi.org/10.1016/j.cirp.2013.05.004).
8. Wang Y, Song R, Yanagimoto J, et al. Effect of heat treatment on bonding mechanism and mechanical properties of high strength Cu/Al/Cu clad composite. *J Alloys Compd* 2019; 801: 573–580. DOI: [10.1016/j.jallcom.2019.06.132](https://doi.org/10.1016/j.jallcom.2019.06.132).
9. Akramifard HR, Mirzadeh H and Parsa MH. Microstructural evolution of roll bonded Al-clad stainless-steel sheets at elevated temperatures. *IJISS*. 2016; 13: 38–44.
10. Jin JY and Hong SI. Effect of heat treatment on tensile deformation characteristics and properties of Al3003/STS439 clad composite. *Mater Sci Eng* 2014; 596: 1–8. DOI: [10.1016/j.msea.2013.12.019](https://doi.org/10.1016/j.msea.2013.12.019).

11. Talebian M and Alizadeh M. Manufacturing Al/steel multi-layered composite by accumulative roll bonding and the effects of subsequent annealing on the microstructural and mechanical characteristics. *Mater Sci Eng* 2014; 590: 186–193. DOI: [10.1016/j.msea.2013.10.026](https://doi.org/10.1016/j.msea.2013.10.026).
12. Lee JE, Bae DH, Chung WS, et al. Effects of annealing on the mechanical and interface properties of stainless steel/aluminum/copper clad-metal sheets. *J Mater Process Technol* 2007; 187–188: 546–549. DOI: [10.1016/j.jmatprotec.2006.11.121](https://doi.org/10.1016/j.jmatprotec.2006.11.121).
13. Manesh HD and Taheri AK. The effect of annealing treatment on mechanical properties of aluminum clad steel sheet. *Mater Des*. 2003; 24: 24617–24622. doi:[10.1016/S0925-8388\(03\)00392-X](https://doi.org/10.1016/S0925-8388(03)00392-X).
14. Kim YK and Hong SI. Influence of interface structure and stress distribution on fracture and mechanical performance of STS439/Al1050/STS304 clad composite. *Mater Sci Eng* 2019; 749: 35–47. DOI: [10.1016/j.msea.2019.02.004](https://doi.org/10.1016/j.msea.2019.02.004).
15. Altan T and Tekkaya AE. *Sheet metal forming: fundamentals*. Detroit: ASM International, 2012.
16. Kim D, Hwang BK, Lee YS, et al. Anisotropic properties of stainless steel-clad aluminum sheet. *AIP Conf Proc* 2010; 1252: 357–360. DOI: [10.1063/1.3457574](https://doi.org/10.1063/1.3457574).
17. Lu R, Liu Y, Yan M, et al. Theoretical, experimental and numerical studies on the deep drawing behavior of Ti/Al composite sheets with different thickness ratios fabricated by roll bonding. *J Mater Process Technol*. 2021; 297: 1–20. Article 117246. doi:[10.1016/j.jmatprotec.2021.117246](https://doi.org/10.1016/j.jmatprotec.2021.117246).
18. Tortorici PCD. Phase formation and interdiffusion in Al-clad 430 stainless steels. *Mater Sci Eng* 1998; 244: 207–2015. DOI: [10.1016/S0921-5093\(97\)00534-0](https://doi.org/10.1016/S0921-5093(97)00534-0).
19. Koseki T, Inoue J and Nambu S. Development of multilayer steels for improved combinations of high strength and high ductility. *Mater Trans* 2014; 55: 227–237. DOI: [10.2320/matertrans.M2013382](https://doi.org/10.2320/matertrans.M2013382).
20. Abedi R and Akbarzadeh A. Bond strength and mechanical properties of three-layered St/AZ31/St composite fabricated by roll bonding. *Mater Des* 2015; 88: 880–888. DOI: [10.1016/j.matdes.2015.09.043](https://doi.org/10.1016/j.matdes.2015.09.043).
21. Pop LD. Research on the optimal regime of recrystallization in 1050 Aluminium alloy. In: *Procedia Manufacturing*. Amsterdam: Elsevier B.V., 2019, pp. 4–7. DOI: [10.1016/j.promfg.2019.02.175](https://doi.org/10.1016/j.promfg.2019.02.175).
22. Chakravarty P, Bátorfi JG and Sidor JJ. Investigation of recrystallization kinetics in 1050 Al alloy by experimental evidence and modeling approach. *Materials* 2023; 16: 5760. DOI: [10.3390/ma16175760](https://doi.org/10.3390/ma16175760).
23. Gu GH, Lee SY, Seo MH, et al. Shear deformation behavior of heterostructured materials: experimental and numerical analyses. *Met Mater Int* 2024; 30: 1256–1269. DOI: [10.1007/s12540-023-01572-x](https://doi.org/10.1007/s12540-023-01572-x).
24. Yang F, Zhu D, Jiang M, et al. Effect of heat treatment on the microstructure, mechanical properties and corrosion resistance of selective laser melted 304L stainless steel. *Acta Metall Sin* 2022; 35: 1688–1702. DOI: [10.1007/s40195-022-01430-6](https://doi.org/10.1007/s40195-022-01430-6).
25. Kuhtz M, Buschner N, Henseler T, et al. An experimental study on the bending response of multi-layered fibre-metal-laminates. *J Compos Mater* 2019; 53(18): 2579–2591. DOI: [10.1177/0021998319835595](https://doi.org/10.1177/0021998319835595).
26. Amanollahi A, Ebrahimzadeh I, Mehdi Raeissi M, et al. Laminated steel/aluminum composites: improvement of mechanical properties by annealing treatment. *Mater Today Commun* 2021; 29: 102866. DOI: [10.1016/j.mtcomm.2021.102866](https://doi.org/10.1016/j.mtcomm.2021.102866).